Melt Memory Effects on Recrystallization of Polyamide 6 Revealed by Depolarized Light Scattering and Small-Angle X-ray Scattering

Jun Kawabata,[1] Go Matsuba,[2] Koji Nishida,[1] Rintaro Inoue,[1] Toshiji Kanaya[1]

[1]*Institute for Chemical Research, Kyoto University, Uji, Kyoto-fu 611-0011, Japan*
[2]*Department of Polymer Science and Engineering, Yamagata University, Yonezawa, Yamagata 992-8510, Japan*

Received 31 July 2010; accepted 6 February 2011
DOI 10.1002/app.34294
Published online 10 June 2011 in Wiley Online Library (wileyonlinelibrary.com).

ABSTRACT: Melt memory effects on recrystallization of polyamide 6 were studied in a length scale from nm to μm using small-angle X-ray scattering (SAXS) and depolarized light scattering (DPLS). The memory effects on recrystallization rate were discussed in terms of the incubation period before nucleation and the half time of the crystallization, which were measures of the nucleation rate and the growth rate, respectively. Both rates are almost independent of the annealing temperature of the melt in the remelting process for the short term annealing below ~ 3 min while they are slowed as the annealing temperature increases for the long term annealing, showing that the relaxation of melt memory takes very long even above the equilibrium melting temperature T_m^0. Extrapolating the incubation period to infinite annealing, time we found that it was very hard to attain the fully relaxed state in polyamide 6 even above the equilibrium melting temperature. This must be due to the strong hydrogen bonding in polyamide 6. We also discuss the memory effects on the final structure after recrystallization based on the SAXS and DPLS profiles. © 2011 Wiley Periodicals, Inc. J Appl Polym Sci 122: 1913–1920, 2011

Key words: crystallization; polyamides; annealing; light scattering; SAXS

INTRODUCTION

Melt memory effects may occur when a semicrystalline polymer is melted and then recrystallized.[1–12] It was found that the time required for the second crystallization (or recrystallization) varied with the temperature of the melt and the time during which the sample was kept in the melt. The memory effects sometimes change crystalline morphology.[12] Normally, the crystallization time decreases as the melt temperature is lowered and the period of melting is shortened.[8,11] The memory effects are usually explained by assuming that some structure in the crystal survives in the melt and acts as a crystal nucleus. It is considered that polymers with strong interactions such as hydrogen bonding have strong memory effects because the retained structure is hard to be relaxed. Among such polymers with strong interactions, polyamides are important polymers in industry, and hence extensive studies have been performed on the melt memory effects.[13–20] Melt memory effects induced by flows, drawing, and processing were also studied by some researchers,[13–17,19–21] which were often called orientation-induced memory effects, because the effects were very important from industrial viewpoints. The effects are often discussed in relation to precursors in flow-induced crystallization of polymers.[22,23] It is considered that the melt memory effects disappear when the polymers are kept at a high temperature above the equilibrium melting temperature T_m^0 in a period longer than the longest relaxation time of the polymer because the imprinted structure in the crystalline state can be relaxed. However, it was reported by Choeinski-Arnault et al. that the memory effects of polyamide survived very long.[18] On the other hand, Vasanthan reported that there were no differences in the crystallization rate between drawn and undrawn polyamides.[19] Thus, the melt memory effect in polyamides is one of the unsolved problems in the research field of polymer crystallization.

The memory effects sometimes affect the final crystalline morphology[6] to change macroscopic properties of the polymers. If the memory effects on polymer morphology appear in nm scale, the lamella crystal stacking is affected, resulting in different mechanical properties. If the effects are in μm scale, the transparency of the polymer is affected. It is important to study the melt memory effects in a wide spatial scale. In this work, we therefore investigated the melt memory effects of thermal history as well as shear flow history on polyamide 6 (Nylon-6) in a length scale from nm to μm using depolarized light scattering and small-angle X-ray scattering.

Correspondence to: T. Kanaya (kanaya@scl.kyoto-u.ac.jp).

EXPERIMENTAL

In the experiments, we used polyamide 6 with relative viscosity of 3.36, corresponding to number average molecular weight M_n of 22,000. The nominal melting temperature determined by differential scanning calorimetry (DSC) was 221°C with heating rate of 10°C/min.

Two-dimensional (2D) depolarized light scattering (DPLS) measurements were carried out using homemade apparatus with He-Ne laser (80 mW, wavelength = 633 nm) as a light source and a 2D screen and a CCD camera as well as a CMOS sensor as detector systems. The details of the DPLS apparatus have been reported in Ref. 24. The ranges of length of scattering vector Q in the experiment using a 2D screen and a CMOS sensor were 3.0×10^{-4} to 3.0×10^{-3} and 2.0×10^{-4} to 2.0×10^{-3} nm^{-1}, respectively, where Q is given by $Q = 4\pi n \sin\theta/\lambda$ (2θ and n being scattering angle and the refractive index of polyamide 6, respectively). In the experiments, we used a value of 1.53 for the refractive index[25] to calculate Q value. The measurements were carried out every 5 s. The scattering intensity was evaluated after correcting for the sensitivity of the detector and the background. For isotropic 2D scattering patterns, we have evaluated circular averaged 1D scattering intensities $I(Q)$ and integrated intensities $I_{\text{integrated}}$ according to the following equation to see the crystallization kinetics;

$$I_{\text{integrated}} = \int_{Q_{\min}}^{Q_{\max}} I(Q) Q^2 dQ \qquad (1)$$

where $Q_{\min}$ and $Q_{\max}$ is the low and upper limits of the integration.

Small-angle X-ray scattering (SAXS) measurements were performed using an apparatus installed at a beam line BL40B2[26] in the synchrotron radiation (SR) facility, SPring-8, in Nishiharima. Wavelength of the incident X-ray was 0.09 nm and the sample-to-detector distance was 1.8 m. A CCD camera (C4880: Hamamatsu Photonics K.K.) with an image intensifier was used as a detector system. The Q range covered in the SAXS measurements was 0.08 to 1.2 nm^{-1}. The exposure time for SAXS measurements was 4 s and the measurements were carried out at 10 s intervals. The scattering intensity was evaluated after correcting the detector efficiency, the background, and the scattering from the empty cell. For isotropic 2D scattering patterns, we have evaluated circular averaged 1D scattering intensities $I(Q)$ and integrated intensities $I_{\text{integrated}}$, similar to the DPLS data.

A Mettler FP-80 was used to control the sample temperature, and a Linkam CSS-450 was also used to control the temperature and shear conditions. The sample was placed between two quartz plates for the DPLS measurements, and between two stainless steel plates with Kapton windows 50 μm thick for the SAXS measurements. The sample thickness was 300 μm for all the measurements. The temperature protocol for the experiments is shown in Figure 1. The sample was heated up to 290°C, which was above the equilibrium melting temperature T_m^0 (= 260°C),[27] from room temperature and held for 1 min. This melting terms the 1st melting in the paper. Then, it was cooled down to 70°C at a cooling rate of 30°C/min for isothermal crystallization. This crystallization terms the 1st crystallization in the paper. After the 1st crystallization, the sample was heated up to various temperatures T_a's above the nominal melting temperature T_m (= 221°C) for the 2nd melting (or remelting), held for various annealing periods t_a and cooled down to 210°C for the successive 2nd crystallization (or recrystallization) to see the melt memory effects on the recrystallization by DPLS and SAXS. The 2nd melting temperatures were in a range between 230 and 290°C, which were always above the nominal melting temperature T_m (= 221°C) and some of which were above the equilibrium melting temperature T_m^0 (= 260°C). The annealing period was between 1 and 540 min. In addition, to see the memory effect of orientation in the 1st crystallization, we have applied a shear flow during the cooling process. After the 1st melting at 290°C, the sample was cooled to 70°C for the 1st crystallization. During the cooling process, we applied a shear flow with shear rate $\dot{\gamma}$ of 36 s^{-1} and shear strain ε of 21,600% on the sample at 215°C. The shearing time corresponding to the shear strain of 21,600% was 6 s. After the 1st crystallization at 70°C, the sample was heated up to a given 2nd melting temperature T_a. The successive experimental procedure to see the melt memory effects was the same as the quiescent crystallization.

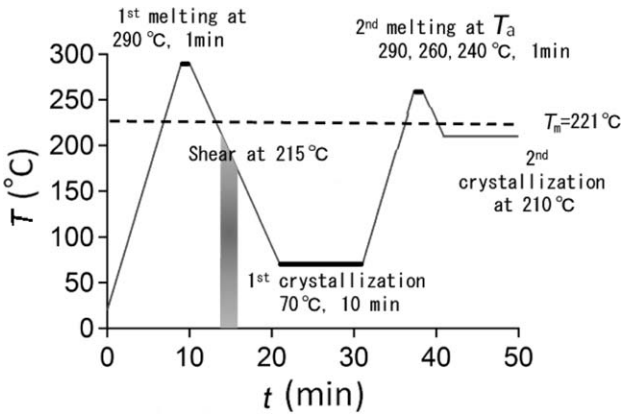

Figure 1 Temperature protocol for 1st melting, 1st crystallization, 2nd melting, and 2nd crystallization of polyamide 6.

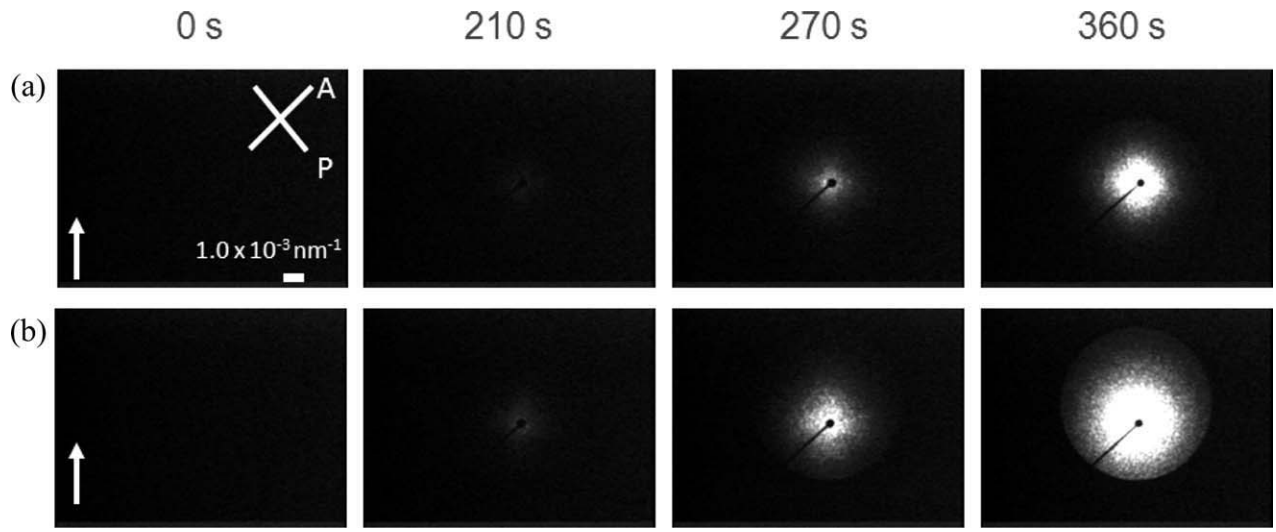

Figure 2 Time evolution of 2D DPLS pattern of polyamide 6 during 2nd crystallization process after 2nd melting at 290°C for 1 min. (a): for quiescently crystallized sample and (b) shear-crystallized sample (shear rate and strain are $\dot{\gamma} = 36\ s^{-1}$ and $\varepsilon = 21{,}600\%$, respectively). Scale bar is $Q = 1.0 \times 10^{-3}\ nm^{-1}$ and A and P show direction of analyzer and polarizer. ↑ Arrows show shear direction.

RESULTS AND DISCUSSION

In the first step, we have examined the melt memory effects in μm scale using DPLS. Figure 2 shows time evolution of 2D DPLS patterns during the 2nd crystallization process after the 2nd melting at 290°C for 1 min. Figure 2(a,b) correspond to the samples crystallized under quiescent and sheared conditions in the 1st crystallization process, respectively. For the original sample (without the 1st crystallization process), the scattering intensity appears ~ 800 s after quenching to the 2nd crystallization temperature (= 210°C), which is much longer than those for the quiescently and shear-crystallized samples. The acceleration of the crystallization rate in the quiescently and shear-crystallized samples clearly shows the melt memory effects. The crystallization rate of the shear-crystallized sample is faster than that of the quiescently crystallized sample although the 2nd melting conditions are the same for both the samples. The result suggests that some structure induced by the shear flow in the 1st crystallization process does not relax during the 2nd melting process, and the unrelaxed structure, which may be oriented in some spatial scale, acts as a crystalline nucleus to accelerate the crystallization rate. It is noted that the 2D DPLS pattern for the shear-crystallized sample does not show any anisotropic scattering pattern [Fig. 2(b)], implying that the oriented structure is smaller than the length scale probed by light scattering (~ μm) or the degree of orientation is too low to be detected. To see the effects of the temperature in the 2nd melting on the 2nd crystallization, we performed experiments for the quiescent and shear-crystallized samples as a function of 2nd melting temperature T_a. As shown in Figure 2(b), 2D DPLS patterns are isotropic for the shear-crystallized sample under the present shear condition, and hence, we calculated integrated scattering intensities $I_{integrated}$ in a Q range from $Q_{min} = 4.0 \times 10^{-4}$ to $Q_{max} = 1.0 \times 10^{-3}\ nm^{-1}$ for evaluation of crystallization kinetics. Time evolutions of the integrated DPLS intensities $I_{integrated}$ during the 2nd crystallization process are shown in Figure 3 after the 2nd melting at 240 and 290°C for the quiescently and shear-crystallized samples. It is evident that the crystallization

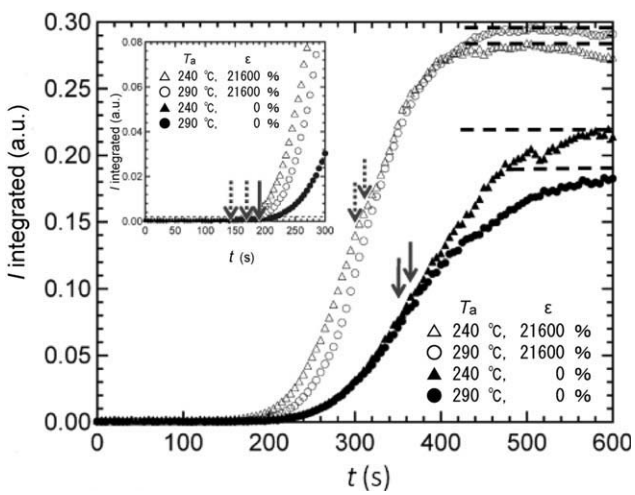

Figure 3 Time evolution of integrated DPLS intensity $I_{integrated}$ during 2nd crystallization process as a function of annealing time. The 2nd melting temperatures are 240 and 290°C for both quiescently and shear-crystallized samples. Arrows show half time of crystallization $t_{1/2}$. Inset is magnification of data in early stage. Arrows in inset show onset times of crystallization (or incubation period t_{inc}).

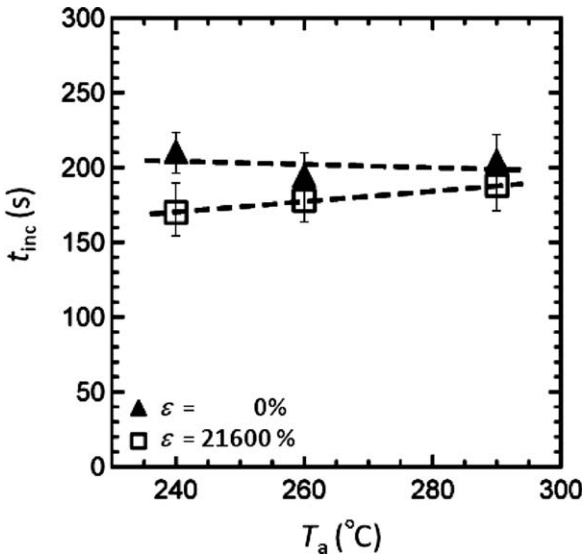

Figure 4 Incubation period t_{inc} determined by DPLS as a function of 2nd melting temperature T_a for both quiescently and shear-crystallized samples. Annealing time t_a is 1 min for all of the measurements.

rate as well as the final scattering intensity after leveling off depend on the 2nd melting temperature and the precrystallization condition. In the following, we will analyze the data more quantitatively.

It is well known that the crystallization process of polymers can be classified into two processes.[28] One is crystalline nucleation process and other is growth process of crystal. The former and the latter were theoretically formulated by Turnbull and Fisher[29] and Lauritzen and Hoffman,[30] respectively. Experimentally, the incubation period t_{inc} before crystal nucleation and the half time of crystallization after the incubation period are mainly dominated by the nucleation rate and the growth rate, respectively. The separation of the crystallization process into these two processes will give us more detailed information on the melt memory effects of polyamide 6.

We first evaluated the incubation period t_{inc} before the crystallization as a measure of crystalline nucleation rate. The DPLS intensities in the early stage of crystallization process were expanded in inset of Figure 3. The incubation periods t_{inc}'s were defined by a time at which the intensity exceeds the detection limit of the DPLS measurements, which were shown by arrows in the inset. The limit is indicated by a dashed line in the inset. The incubation periods t_{inc}'s thus evaluated are plotted in Figure 4 as a function of the 2nd melting temperature T_a for the quiescently and shear-crystallized samples. Comparing t_{inc}'s between the shear-crystallized and quiescently crystallized samples, the t_{inc} of the shear-crystallized sample seems slightly shorter than that of the quiescently crystallized one even after melting above the equilibrium melting temperature T_m^0 (= 260°C). This suggests that the nucleation rate is accelerated by some structure induced by the shear, which can survive even above the equilibrium melting temperature T_m^0 and act as nucleating agent. It is interesting to point out that the incubation period t_{inc} is almost independent of the temperature in the 2nd melting process. Normally, the melt memory effects depend on the remelting temperature very much.[4] Does this result mean that the structure memory imprinted during the 1st crystallization almost disappears? As shown by Chocinski-Arnault,[11] the relaxation of memory effects in polyamides takes very long even above the melting temperature T_m. We therefore examined the incubation period t_{inc} in the 2nd crystallization process as a function of the annealing time t_a in the 2nd melting process at T_a = 240, 260, and 290°C. The result is shown in Figure 5 for the quiescently crystallized sample. The incubation period t_{inc} increased as both the annealing time t_a and temperature T_a increased in the 2nd melting process. The shear-crystallized sample also shows large effects of the annealing time on the incubation period as seen in Figure 6. These results clearly show that the memory imprinted during the 1st crystallization process cannot be erased in the 2nd melting process even above the equilibrium melting temperature T_m^0 for 600 min. To predict the incubation period t_{inc} at infinite annealing time ($t_a = \infty$), we replotted the incubation time against inverse of annealing time t_a^{-1} in inset of Figure 6. In the short time region below $t_a \sim 200$ min ($t_a^{-1} > 0.05$ s^{-1}), the t_a^{-1} dependence of the incubation period time t_{inc} is very weak, whereas it becomes steep in the long time region above $\sim$ 200

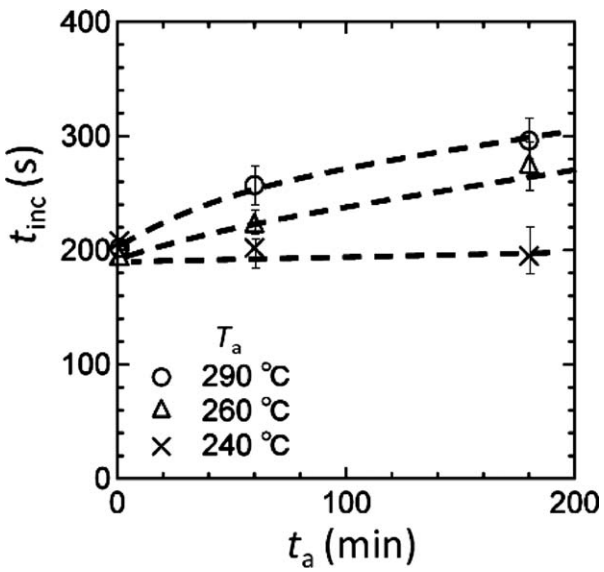

Figure 5 Annealing time t_a dependence of incubation period t_{inc} during 2nd crystallization process at 210°C for quiescently crystallized samples. The 2nd melting temperatures T_a are 240, 260, and 290°C.

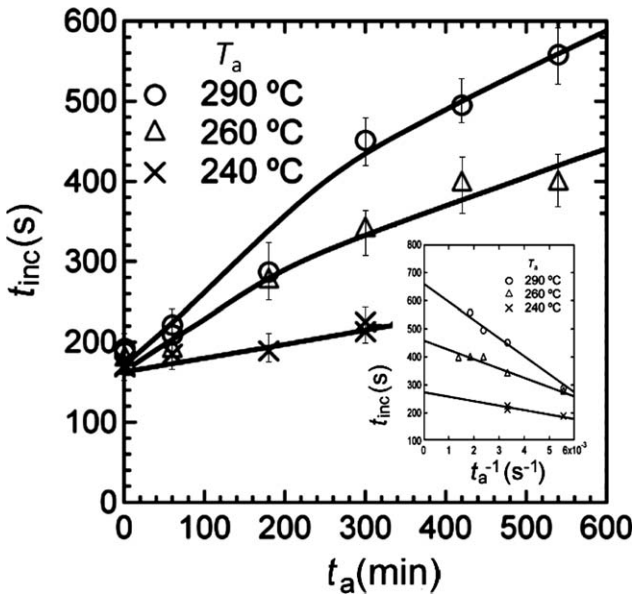

Figure 6 Annealing time t_a dependence of incubation period t_{inc} during 2nd crystallization process at 210°C for shear-crystallized samples. The 2nd melting temperatures are 240, 260, and 290°C. In inset incubation period t_{inc} is plotted versus inverse of annealing time t_a^{-1}. Data at $t_a = 1$ and 60 min are not included in inset.

min ($t_a^{-1} < 0.05$ s^{-1}) and the incubation period t_{inc} seems to linearly increase with t_a^{-1}. Extrapolating to $1/t_a = 0$ according to the linear relation, the infinite incubation period at each annealing temperature does not come to the same value, showing that it is hard to attain the fully relaxed state in the polyamide 6 in the present annealing condition. It is expected that the strong memory effect must be caused by hydrogen bonding in polyamide 6.

In the next, we focus on the growth rate of crystals. For this purpose, we evaluated the half time of crystallization from the time evolution of the DPLS intensity in Figure 3. The arrows in the figure show the apparent half times $t_{1/2}$ which is defined as a time at which the DPLS intensity is half of the final value after leveling off. It is noted that the $t_{1/2}$ includes the incubation period t_{inc}, and hence, we have subtracted the incubation period t_{inc} from the apparent half time $t_{1/2}$ to obtain the half time $t_{1/2,G}$ which is a measure of the crystal growth rate. The evaluated half time $t_{1/2,G}$ is plotted against the annealing time t_a in the 2nd melting process at $T_a =$ 240, 260, and 290°C in Figure 7 for the shear-crystallized sample. For the very short annealing time, the $t_{1/2,G}$ is almost the same for various T_a's, whereas the difference in the $t_{1/2,G}$ becomes large with increasing t_a. Similar results were obtained for the quiescently crystallized samples although the data are not shown here. The annealing time t_a and annealing temperature T_a dependences of the $t_{1/2,G}$ which corresponds to the crystal growth rate are very similar to those of the incubation periods (Fig. 6), meaning that the melt memory effects in the polyamide 6 accelerate the crystal nucleation process as well as the crystal growth rate in a similar manner. It is not a usual result. Generally speaking, the melt memory effects accelerate the nucleation process but not the growth rate because some persist structures may act as crystalline nuclei. However, the present result shows that the memory effects accelerate not only the nucleation rate but also the crystal growth rate. In the growth process, a part of polymer chains (stem) must attach the crystal surface, which is the secondary nucleation process in terms of Lauritzen-Hoffman theory.[30] In the attaching process, a part of polymer chain must align or rearrange the conformation along the crystal surface. In this process, the local oriented structure retained in polyamide 6 could work as rearranged part to accelerate the growth rate. This is one of possible explanations for the acceleration of the growth rate. Recently, Martins et al.[21] studied crystallization from fully relaxed melt and the presheared melt of isotactic polypropylene (iPP) and found that no significant changes in the nucleation density occurred when relaxed and presheared melts crystallized at the same temperature while the crystallization rate from the presheared melt was faster that that from the fully relaxed melt. They showed that the crystallization rate should increase due to the viscosity decrease associated to melt shearing. The decrease in the viscosity is another possible explanation for the acceleration in the crystal growth rate of the shear-crystallized polyamide 6.

In the DPLS measurements, we focus on the memory effects in the recrystallization process in μm

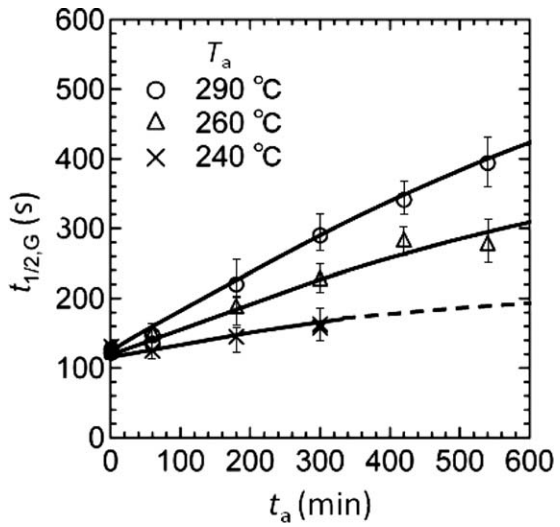

Figure 7 Annealing time t_a dependence of $t_{1/2,G}$ in the 2nd crystallization at 210°C for shear-crystallization samples. The 2nd melting temperatures are 240, 260, and 290°C.

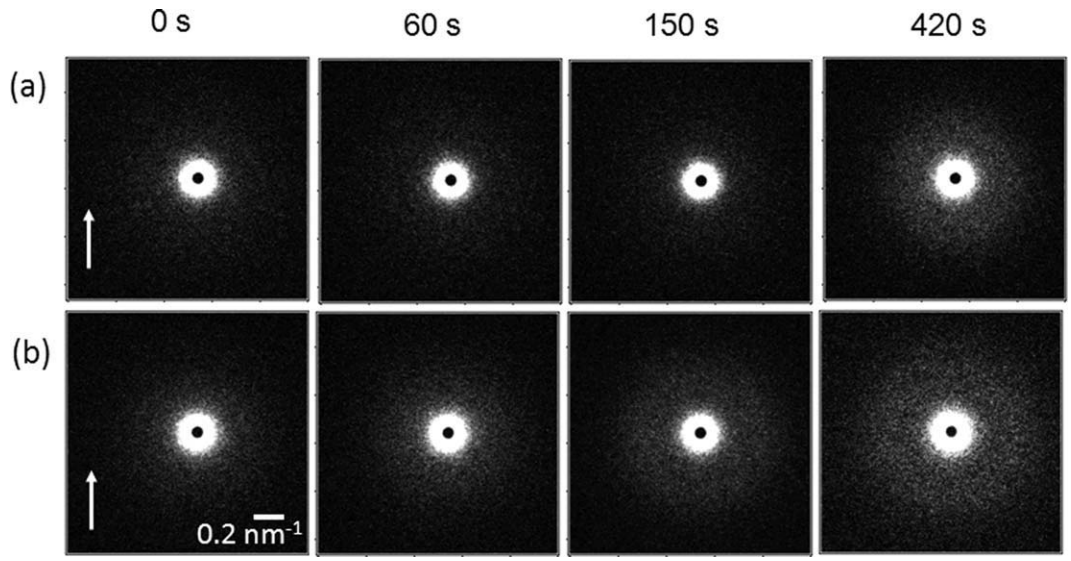

Figure 8 Time evolution of 2D SAXS pattern during 2nd crystallization process at 210°C after 2nd melting at 290°C for 3 min. (a) for quiescently crystallized sample and (b) shear-crystallized sample (shear rate and strain are $\dot{\gamma} = 36\ s^{-1}$ and $\varepsilon = 21{,}600\%$, respectively). Scale bar is $Q = 0.2\ nm^{-1}$ and arrows show shear direction.

scale. The structure formation in μm scale must be related to that in nm to several tens nm scale. Hence, we also studied the melt memory effects on the crystallization process in nm scale using small-angle X-ray scattering (SAXS). We performed time-resolved measurements on the structure formation in the 2nd crystallization process after the 2nd melting process (Fig. 1). In the SAXS experiments, the annealing time in the 2nd melting process was fixed at 3 min, and the measurements were done on both the quiescently and shear-crystallized samples. In Figure 8, 2D SAXS patterns are shown for the quiescently and shear-crystallized samples during the 2nd crystallization process after the 2nd melting at 290°C for 3 min. Any anisotropic scattering patterns were not observed in the SAXS measurements for the shear-crystallized sample, but the crystallization rate for the shear-crystallized sample was faster than that for the quiescent crystallized one. The results are very similar to those of the DPLS ones, suggesting that some structure induced by the shear flow in the 1st crystallization process survived in the 2nd melting and accelerated the crystallization rate. We expected that the unrelaxed structure was oriented, but no anisotropic scattering patterns were observed in either the DPLS or SAXS patterns. Probably the degree of orientation in the unrelaxed structure is very low, at least in the spatial scale studied in this experiment. Another possibility is that the oriented structure is smaller than the spatial scale probed by SAXS (~ 5 nm) but is not plausible because the SAXS limit is less than the critical nuclear size (~ 10 nm).[1] Because of the nonoriented feature of the 2D SAXS patterns, we employed the 1D circular averaged intensity $I(Q)$ and/or the integrated intensity $I_{integrated}$ in a Q range from $Q_{min} = 0.1$ to $Q_{max} = 1.0$ nm^{-1} [Eq. (1)] in the later discussions.

On the basis of the time evolution of integrated SAXS intensity, we estimated the incubation period t_{inc} and the half time of crystallization $t_{1/2,G}$ in the same manner as the DPLS measurements (Fig. 3). The evaluated incubation period t_{inc} and the half time $t_{1/2,G}$ are shown as a function of the 2nd melting temperature in Figures 9 and 10, respectively, for both of the quiescently and shear-crystallized samples. The incubation period t_{inc} for the shear-

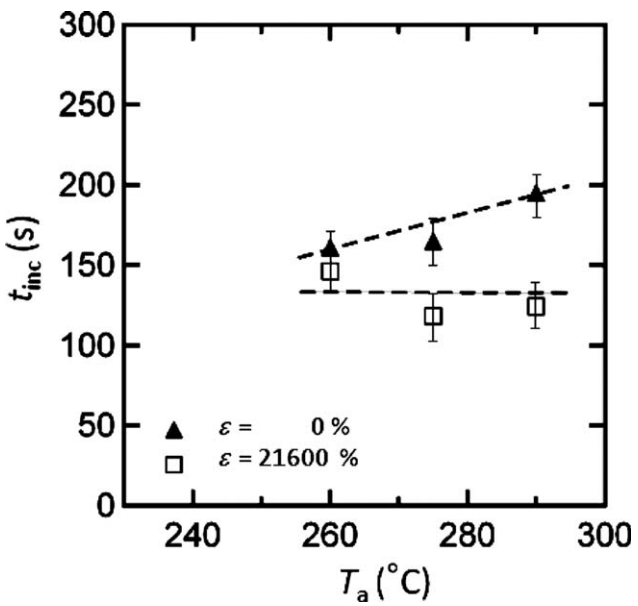

Figure 9 Incubation period t_{inc} determined by SAXS as a function of 2nd melting temperature T_a for both quiescently and shear-crystallized samples.

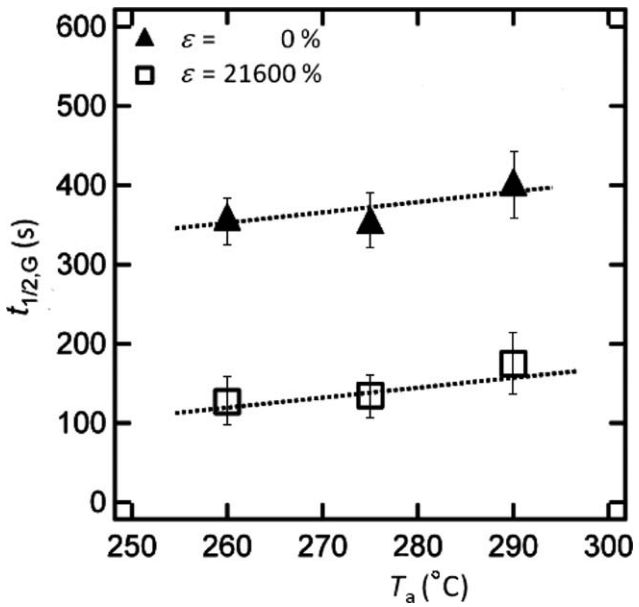

Figure 10 Half time $t_{1/2,G}$ determined by SAXS as a function of 2nd melting temperature T_a for both quiescently and shear-crystallized samples.

crystallized sample is shorter than that for the quiescently crystallized one and is almost independent of the annealing temperature for the 3 min annealing. These results are qualitatively the same as the DPLS ones. In addition, the half time $t_{1/2,G}$ also shows the same tendencies: the $t_{1/2,G}$ for the shear-crystallized sample is shorter than that for the quiescent crystallized one and almost independent of the melting temperature for the 3 min annealing. The memory effects on the recrystallization process in nm to several tens nm scale are the same as those in μm scale probed by DPLS, suggesting that the μm scale structure formation is dominated by the nm structure formation in polyamide 6.

In the above discussion, we mainly focused on the crystallization rate, dividing into the crystal nucleation process and the growth process. In the following, we examined the melt memory effects on the structure itself in a scale from nm to μm based on the SAXS and DPLS data. To compare the shapes of the scattering profiles, we first normalized the integrated DPLS and SAXS intensities to the final value after leveling off. In Figure 11(a), the normalized DPLS profiles of the quiescently crystallized samples are plotted after recrystallization following the 2nd melting process at T_a = 260, 275, and 290°C for 3 min. The profiles are identical within the experimental accuracy, showing that the structure does not depend on the 2nd melting temperature, similar to the dependence of the nucleation rate on the 2nd melting temperature for short annealing time (Fig. 4). In Figure 11(b), we plot the normalized DPLS profiles for the quiescently crystallized samples annealed at 290°C for 3 and 300 min to see the annealing time effect and the profile for the share-crystallized sample annealed at 290°C for 3 min to study the shear effect. The difference of profiles between the long and short annealed samples is very small, implying that the annealing time effect on the structure is negligible. On the other hand, the shear-crystallized sample shows high intensity in the low Q range below about 6×10^{-4} nm^{-1}, suggesting that the shear flow induces the density fluctuations in μm scale which cannot be erased in the 2nd annealing process above the equilibrium melting temperature T_m^0. This may affect the transparency of the samples. In Figure 12, the normalized SAXS

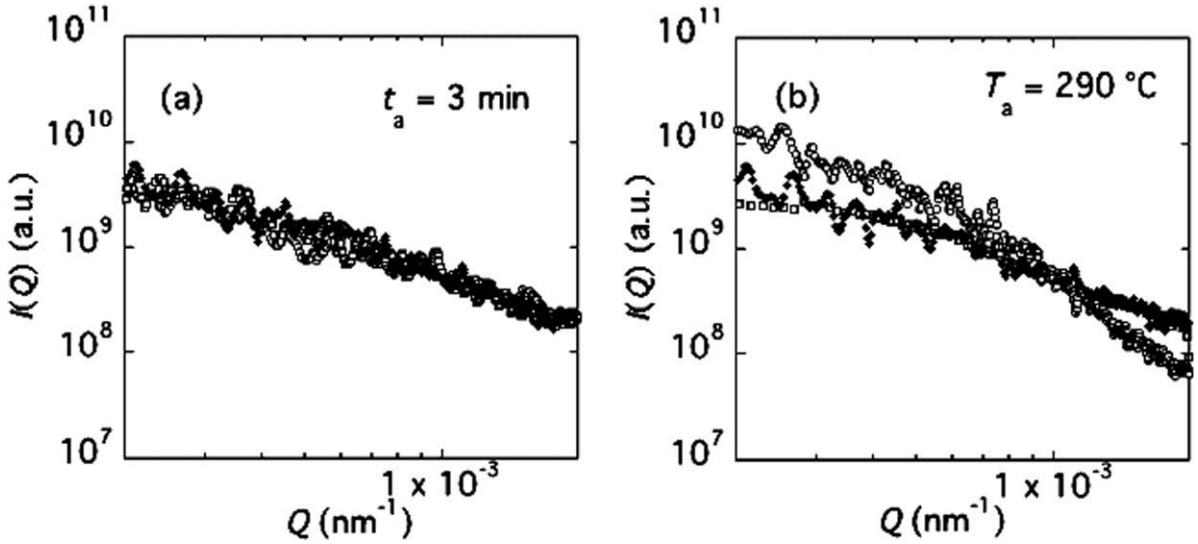

Figure 11 DPLS profiles after 2nd crystallization. a: the quiescently crystallized samples annealed at T_a = 260°C (circle), 275°C (square), and 290°C (closed diamond) for t_a = 3 min. b: the quiescently crystallized samples annealed at 290°C for t_a = 3 min (closed diamond) and 300 min (square) and the shear-crystallized samples annealed at 290°C for t_a = 3 min (circle).

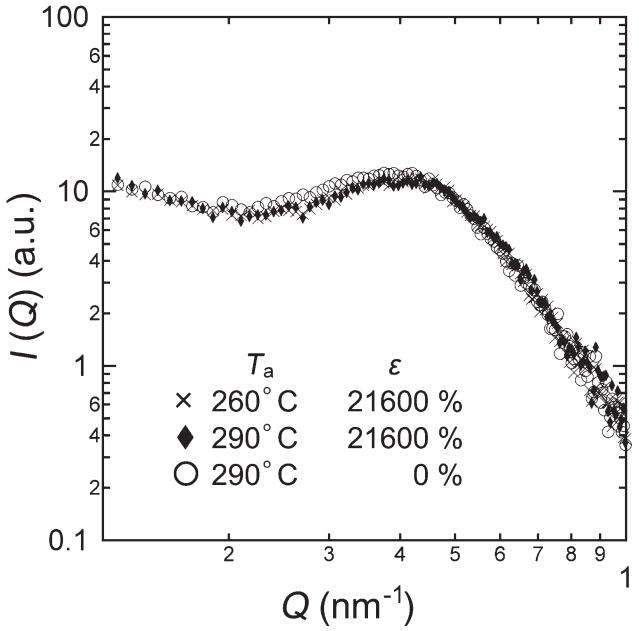

Figure 12 SAXS profiles after 2nd crystallization for quiescently crystallized samples annealed at 290°C (circle) and the shear-crystallized samples annealed at 260 (cross) and 290°C (diamond). The annealing time t_a in the 2nd melting was 3 min for all the measurements.

profiles are shown after recrystallization for the quiescently crystallized samples annealed at 290°C and for the shear-crystallized samples annealed at 260 and 290°C in the 2nd melting process. The profiles are almost identical, showing that the structure in nm scale is not affected by the memory effect so much, at least in the present crystallization and melting conditions.

CONCLUSIONS

In the work we have studied the melt memory effects on the recrystallization of polyamide 6 in a length scale from nm to μm using SAXS and DPLS. The recrystallization rate after the 2nd melting was discussed in terms of the incubation period t_{inc} and the half time $t_{1/2,G}$ of crystallization, which were measures of the nucleation rate and the growth rate, respectively. It was found that both the rates were almost independent of the 2nd melting temperature in short annealing period less than ~ 3 min, whereas the rates in the long annealing period decrease as the 2nd melting temperature increases. The results clearly show that the relaxation of structure imprinted during the 1st crystallization takes very long time probably due to the strong hydrogen bonding. It was surprising that extrapolating the incubation period to the infinite annealing time it did not reach the same value even above the equilibrium melting temperature T_m^0, showing that it is very hard to attain the fully relaxed state in polyamide 6 even above the equilibrium melting temperature. We also studied the memory effects on the final structure after the recrystallization. It was found that the memory effects are negligible in the structure for the quiescently crystallized samples in a spatial scale from nm to μm. The effects of the shear in the 1st crystallization were retained after the 2nd melting as density fluctuations in μm scale.

The authors are grateful to Ube Industries Ltd., Japan, for supplying the polyamide 6 for this work.

References

1. Wunderlich, B. Macromolecular Physics; Academic Press: New York, 1957; Vol. 2, pp 52–70.
2. Banks, W.; Gordon, M.; Sharples, A. Polymer 1963, 4, 289.
3. Banks, W.; Sharples, A. Makromol Chem 1963, 67, 42.
4. Fillon, B.; Wittmann, J. C.; Lotz, B.; Thierry, A. J Polym Sci Part B: Polym Phys 1993, 31, 1383.
5. Fillon, B.; Lotz, B.; Thierry, A.; Wittmann, J. C. J Polym Sci Part B: Polym Phys 1993, 31, 1395.
6. Fillon, B.; Thierry, A.; Wittmann, J. C.; Lotz, B. J Polym Sci Part B: Polym Phys 1993, 31, 1407.
7. Ziabicki, A.; Alfonso, G. C. Colloid Polym Sci 1994, 272, 1027.
8. Alfonso, G.; Ziabicki, A. Colloid Polym Sci 1995, 273, 317.
9. Supaphol, P.; Spruiell, J. E. J Appl Polym Sci 2000, 75, 337.
10. Supaphol, P.; Lin, J.-S. Polymer 2001, 42, 9617.
11. Haefele, A.; Heck, B.; Hippler, T.; Kawai, T.; Kohn, P.; Strobl, G. Eur Phys J E 2005, 16, 217.
12. Mamun, A.; Umemoto, S.; Okui, N. Macromolecules 2007, 40, 6296.
13. Khanna, Y. P.; Reimschuessel, A. C. J Appl Polym Sci 1988, 35, 2259.
14. Khanna, Y. P.; Reimschuessel, A. C.; Banerjie, A.; Altman, C. Polym Eng Sci 1988, 28, 1600.
15. Khanna, Y. P.; Kumar, R.; Reimschuessel, A. C. Polym Eng Sci 1988, 28, 1607.
16. Khanna, Y. P.; Kumar, R.; Reimschuessel, A. C. Polym Eng Sci 1988, 28, 1612.
17. Khanna, Y. P.; Kuhn, W. P.; Macur, J. E.; Messa, A. F.; Murthy, N. S.; Reimschuessel, A. C.; Schneider, R. L.; Sibilla, J. P.; Signorelli, A. J.; Taylor, T. J. J Polym Sci Part B: Polym Phys 1995, 33, 1023.
18. Chocinski-Arnault, L.; Gaudefroy, V.; Gacougnolle, J. L.; Riviere, A. J Macromol Sci Phys 2002, 41, 777.
19. Vasanthan, N. J Appl Polym Sci 2003, 90, 772.
20. Su, K.-H.; Lin, J.-H.; Lin, C.-C. J Mater Process Technol 2007, 192, 532.
21. Martins, J. A.; Weidong, Z.; Brito, A. M. Polymer 2010, 51, 4185.
22. Somani, R. H.; Yang, L.; Hsiao, B. S. Phys A 2002, 304, 145.
23. Azzurri, F.; Alfonso, G. C. Macromolecules 2008, 41, 1377.
24. Nishida, K.; Ogawa, H.; Matsuba, G.; Konishi, T.; Kanaya, T. J Appl Cryst 2008, 41, 723.
25. Brabdrup, J.; Immergut, E. H.; Grulke, E. A., Eds. Polymer Handbook; Wiley-Interscience: NewYork, 1999; Vol. 128.
26. Shimizu, N.; Inoue, K. SPring-8 Beamline Handbook; 2003; Vol. 90.
27. Gogolewski, S.; Gasiorek, M.; Czerniawska, K.; Pennings, A. J Colloid Polym Sci 1982, 260, 859.
28. Mandelkern, L. Crystallization of Polymers—Kinetics and Mechanisms; Cambridge University Press: Cambridge, 2002; Vol. 2, pp 11–43.
29. Turnbull, D.; Fisher, J. C. J Chem Phys 1949, 17, 71.
30. Lauritzen, J. I.; Hoffman, J. D. J Appl Phys 1973, 44, 4340.